

Multi-year diagnosis of unpredictable fouling occurrences in a full-scale membrane bioreactor

A. L. Carlson , G. T. Daigger , N. G. Love  and E. Hart

ABSTRACT

The membrane bioreactor (MBR) at the Traverse City Regional Wastewater Treatment Plant has experienced sudden and unpredictable periods of substantial permeability decline since 2011. Early observations detected irregularly-shaped Gram-positive bacteria that correlated with plant upsets. Use of biomolecular techniques, such as DNA sequencing of laboratory isolates and the mixed liquor microbial community, and fluorescent *in situ* hybridization, identified the dispersed organisms as members of the genus *Staphylococcus*. However, *Staphylococcus* species were consistently present during normal operation and therefore were more likely to be an indicator of the upset, not the cause. The results suggest that these microorganisms are responding to specific influent wastewater constituents. We chemically analysed seven mixed liquor samples from periods of permeability decline in 2017 and 2018, and four samples from a period of normal operation. During upset conditions, the total carbohydrate content exceeded that of normal operation by 40%. Additionally, mixed liquor calcium concentrations were 65% above normal during the upset in 2017. It is hypothesized and supported through multivariate statistical analysis and estimation of specific resistance to filtration values that a calcium-intermediated polymer bridging mechanism with extracellular polymeric substance constituents is a major contributor to fouling and permeability disruptions in the Traverse City MBR.

Key words | biomolecular analysis, cation analysis, dispersed bacteria, MBR fouling, specific resistance to filtration, wastewater

HIGHLIGHTS

- This study investigated fouling drivers at a full-scale MBR plant experiencing an unexplainable problem over many years.
- The study unraveled multiple hypotheses, both chemical and biological in nature.
- Evidence for the drivers of permeability problems points to non-domestic sources.
- Chemical monitoring was initiated, and specific tools were used to enhance the plant's ability to detect impending upsets.

INTRODUCTION

Membrane bioreactors (MBRs) have become increasingly popular in wastewater treatment practice since the end of the 20th century. They combine the biological processes of activated sludge and liquid–solid separation through size exclusion by a membrane to remove wastewater pollutants and produce a high-quality effluent (Meng *et al.* 2017). MBR technology has been increasingly

implemented in wastewater treatment plants throughout China, Europe and the United States because of its inherent benefits, such as an easily controllable solids retention time, ammonia reduction capacity and enhanced biological phosphorus removal potential (Lesjean *et al.* 2002; Meng *et al.* 2017). One such MBR plant of particular interest is the Traverse City Regional

A. L. Carlson 
G. T. Daigger  (corresponding author)
N. G. Love 
Department of Environmental Engineering,
University of Michigan,
1351 Beal Avenue, Ann Arbor, MI 48109,
USA
E-mail: gdaigger@umich.edu

E. Hart
Traverse City Regional Wastewater Treatment
Plant,
606 Hannah Avenue, Traverse City, MI 49686,
USA

Wastewater Treatment Plant (TCRWWTP) located in northern Michigan.

Completed in 2004, TCRWWTP is one of the first plants in the world to operate an MBR at continuous flow and at significant scale (32,000 m³/day). The plant at Traverse City serves a wide array of customers, from municipal (90–95%) to industrial (5–10%). The TCRWWTP consists of screening/grit removal, primary clarification and MBR activated sludge followed by UV disinfection. Mean cell residence time is seasonally varied to promote nitrification (5–15 days), and the mixed liquor suspended solids (MLSS) inventory ranges from 1.50 to 8.50 g/L. Secondary effluent is discharged to Boardman Lake, which ultimately drains into the Grand Traverse Bay on northern Lake Michigan. Waste activated sludge (WAS) is thickened in a gravity belt concentrator and combined with primary sludge prior to anaerobic digestion. Digested sludge thickening and storage facilities are provided, and digested sludge is land applied.

Prior to 2011, marking nearly eight years of operation, the MBR operational parameters, permeability and transmembrane pressure (TMP) had a standard and reproducible differential throughout 12-min permeation cycles (Blair 2012). In 2011, the treatment plant experienced a sudden and substantial membrane fouling event – unexpected, rapid decline in membrane permeability and TMP that increased throughout the permeation cycle, and an exponential increase in time-to-filter (TTF). Plant operators observed a characteristic slimy coating on the membrane surfaces, as well as increased counts of globular zoogloal organisms during and after the plant upset. A third-party review of sludge samples in 2011 revealed substantially increased amounts of dispersed bacteria (Blair 2012). Moreover, these bacteria were Gram-positive – an unusual characteristic for municipal mixed liquors, which normally contain much higher Gram-negative populations (Jenkins *et al.* 2004)—and had an irregular bent rod morphology that plant operators termed comma-shaped. Membrane upsets have persisted periodically since 2011, occurring once or twice a year at random times (see Table SI-I in the Supplementary Information for full timeline of events). TCRWWTP has been able to manage these events with increased ferric dosing, recovery cleans, air scouring and relaxation or backpulsing of the membrane, although the duration and magnitude of upsets continues to be difficult to predict and makes preparation unrealistic. Plant staff initially hypothesized that permeability decline was directly related to the dispersed bacteria population that appeared based on observations of mixed liquor microbiology and measurement of biocake resistance on the

membrane surface (Blair 2012). This paper relays the experimental and evaluative process that ensued to evaluate their assertion.

The investigation began in 2016 with a review of historical operational data to establish baseline mass loadings and seasonal trends for commonly monitored wastewater constituents. When typical and upset plant conditions were compared, there was insufficient evidence that a single measured mass load was correlated with membrane permeability decline. A March 2017 permeability and subsequent dispersed bacterial growth event allowed concurrent experimental testing on the MBR mixed liquor. Four rounds of sampling occurred: two characterized by MBR permeability decline, and two during normal operation. Once experimental data were analysed, evidence supported shifting the hypothesis away from a microbiological cause for MBR upsets to chemical and physical mechanisms that involve components previously unmeasured at the full plant scale.

This case study is organized to convey both experimental evidence and the thought process that led to identifying the cause of MBR upset. The first section of this paper is dedicated to establishing why the initial hypothesis was unsupported and the rationale for a secondary hypothesis. The second section then explains the experimental outcomes and analyses used to evaluate the second hypothesis. A roadmap detailing the transition between the unsupported initial hypothesis to an alternative hypothesis that led to the conclusions of this study is shown in Figure 1.

The hypothesis development process was used to unravel a challenge occurring to a significant North American MBR system. For use in MBR assessments, it provides a framework to assist current and future MBR plant operations. We applied a combination of chemical and biomolecular techniques to investigate the nature of the dispersed organisms relative to permeability upsets, and developed a hypothesis regarding the actual drivers of permeability disruptions in this full-scale wastewater treatment MBR. The outcomes of this study provide useful methodological and analytical information.

MATERIAL AND METHODS

Plant data, activated sludge samples, enrichments and culture isolation

Activated sludge samples were collected during periods when the TCRWWTP was performing normally, and also

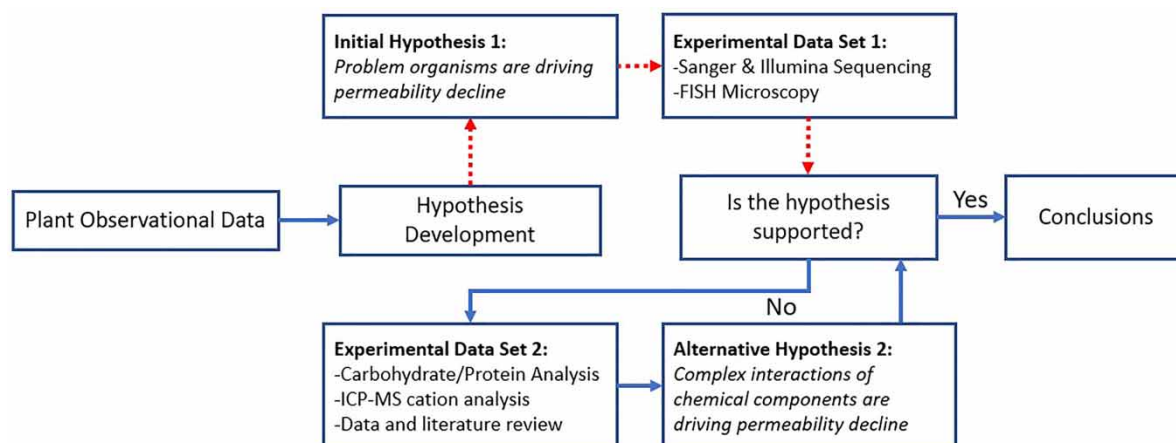


Figure 1 | Project roadmap detailing the complicated hypothesis development process from the initial hypothesis based on plant personnel observations to an alternative hypothesis after exploratory data collection. Dotted line indicates direction of initial experimentation and solid line indicates the ultimate concluding path.

when it was experiencing reduced membrane permeability. Sampling occurred in August and September 2017 (baseline operation without permeability issues, sample IDs designated C for control), and during upset events that occurred in March/April 2017 and January/March 2018 (sample IDs designated RP for reduced permeability). A summary of these sampling events, along with sample identifying codes, is given in Table SI-I. Furthermore, historical data performed by TCRWWTP staff using [Standard Methods \(2017\)](#), including 5-day biochemical oxygen demand (BOD₅), total suspended solids (TSS), total ammonia-nitrogen and total phosphorus were collected and reviewed for the plant's influent, primary effluent and secondary effluent for each outbreak from 2011 through to the end of 2018.

Activated sludge samples (RP-TC-ML 1–5) were enriched by exploiting the dispersed nature of the problem bacteria. Several 2-L samples were taken from the TCRWWTP aeration basin. A portion of the original sample was separated and allowed to gravity settle for several hours. The supernatant, after the settling phase, was presumed to have a higher abundance of the problem organisms based on their observed preference for the planktonic state. The selected dispersed biomass was further concentrated from the supernatant by centrifugation for 10 min at low speed to avoid cell destruction (4,000× *g*), transferred to a 50% v/v glycerol solution and frozen at −20 °C. Bacterial colonies were cultured from these enriched samples (sample IDs: RP-TC-ML E1–E5) on Reasoner's 2A (R2A, Teknova) media using a sterile T-streaking technique. Each individual enriched sample was then re-streaked three times to capture isolates ($n = 13$). The less

concentrated micronutrient profile of the R2A media was selected to decrease bias towards fast-growing heterotrophs and provide an opportunity for slower-growing microorganisms to grow.

Biomolecular analyses

DNA was extracted from the isolated colonies using a crude extraction technique of extreme cyclical heating (5 min at 95 °C) and freezing (−80 °C) in a Mastercycler Thermocycler (Eppendorf AG, Hamburg, Germany), according to [Miller *et al.* \(1999\)](#). The nearly full-length 16S rRNA gene was amplified by polymerase chain reaction (PCR) using forward primer 8F and reverse primer 1387R ([Chiao *et al.* 2014](#)). The PCR conditions were: 10 s at 98 °C followed by 30 cycles of 98 °C for 1 s, 62 °C for 5 s, 72 °C for 21 s, followed by 72 °C for 1 min and held at 4 °C until sample retrieval. PCR products were pre-processed through gel electrophoresis and fully cleaned using Qiaquick Gel Extraction Kit (Qiagen) before submission to the University of Michigan Advanced Genomics Sequencing Core (Ann Arbor, MI, USA) for Sanger Sequencing. Forward and reverse sequence reads were entered into BLAST (NCBI) for species identification with near 100% sequence alignment.

Mixed liquor samples collected during periods of stable plant operation and an upset period (sample IDs: C-TC-FISH 1–2, RP-TC-ML-FISH 3–6) were analysed by fluorescent *in situ* hybridization (FISH). Mixed liquor (10 mL) from the aerobic zone of TCRWWTP's aeration basin was centrifuged for 10 min at 4,000× *g*, washed twice in 5 mL phosphate buffer solution and fixed with 2.5 mL of absolute

ethanol. Fixed samples were stored in a -20°C freezer. FISH DNA probes were designed for each of the three Gram-positive bacterial genera found during the previous Sanger Sequencing process (*Microbacterium*, *Micrococcus* and *Staphylococcus*) using DECIPHER (Wright *et al.* 2014); the probe sequences are provided in Table SI-II. Interference for each individual probe was checked using the Ribosomal Database Project (RDP) (Cole *et al.* 2014). A probe was considered viable if it had a 100% sequence match with the genera in DECIPHER, a high specificity and the lowest potential cross reaction according to RDP. These sequences were then tested for mismatches against our known Sanger sequences and were found to have none. At this point, the three probes had highly specific and identifiable sequences. Finally, the laboratory isolates were used as a positive control for FISH to confirm that the probe was fluorescing with the desired bacterial target.

Fixation, permeabilization and hybridization were completed according to the FISH Handbook for Biological Wastewater Treatment (Nielsen *et al.* 2009). An optimal formamide concentration was needed to first ensure adequate specificity with positive controls and *in situ* samples. We estimated the workable concentration of formamide for each probe using DECIPHER (30% for *Microbacterium* and *Staphylococcus* probes, and 15% for the *Micrococcus* probe). The final hybridization buffer solution was determined using the recipe in Nielsen *et al.* 2009. The entire pre-processing, hybridization and microscopy of TCRWWTP mixed liquor samples were verified with a universal bacteria probe, Bact-338, and a negative control (nonsense) probe, Non-EUB338.

DNA was extracted from unaltered mixed liquor samples collected during the permeability declines of 2017 and 2018 (sample IDs: RP-TC-ML Weeks 1–4, RP-TC-ML Weeks 9–10) and a period of normal operation (sample ID: C-TC-ML Weeks 5–8). Mixed liquor was vacuum filtered through a $0.2\ \mu\text{m}$ polycarbonate filter (Millipore Sigma) and digested in a phenol–chloroform–isoamyl alcohol (25:24:1) solution according to the protocol by Hill *et al.* (2015). The mixture underwent bead beating for 2 min at room temperature, followed by centrifugation at $12,500\times g$ three times where the DNA-rich aqueous phase was captured and purified using the Maxwell[®] LEV Blood DNA kit (Promega). The extracted DNA was sequenced using the Illumina MiSeq 16S rRNA gene platform to reveal relative changes to the entire microbial community in the MBR during plant upsets. PCR conditions and barcoded dual-index paired-end primers targeting a 250 base pair hypervariable segment of the V4 region of the 16S rRNA gene were used

to amplify the DNA, according to the procedure detailed in Kozich *et al.* (2013). Sequencing results of the larger microbial community from March and April 2017, August and September 2017, and January 2018 samples were processed, aligned to a reference database (SILVA Release 132) (Pruesse *et al.* 2007) and analysed using mothur (version 1.42.0). Erroneous sequence fragments and chimeras were removed with mothur quality control algorithms (Kozich *et al.* 2013; Schloss *et al.* 2009) and the remaining sequences were annotated and clustered into operational taxonomic units (OTUs). Relative abundance was determined as the number of individual OTUs divided by the total number of community OTUs.

Mixed liquor chemical and physical analysis

Mixed liquor samples from the plant's aeration basin were analysed to determine the biochemical constituents of observed slime that formed during a permeability upset in March/April 2017 (sample IDs: RP-TC-ML Weeks 1–4), as well as a period of normal operation in August/September 2017 (sample IDs: C-TC-ML Weeks 5–8). Total carbohydrates and total protein concentrations were analysed in triplicate using the DuBois and the Thermo Fisher micro-Bicinchoninic Acid (micro BCA) methods, respectively (DuBois *et al.* 1956; Item #23235, Thermo Scientific). The DuBois method was slightly altered to include additional digestion with sulfuric acid and 80% phenol at 90°C for 5 min. Colorimetric measurements were taken on a spectrophotometric plate reader at 490 nm, and concentration was calculated from an acid/phenol-digested dextrose standard curve. Total protein content was solubilized through base digestion with 1 N sodium hydroxide at 100°C , according to Lowry *et al.* (1951), diluted by a factor of 20 and measured at 562 nm using a microplate reader. Total protein concentration was calculated from correlation to a base-digested bovine serum albumin standard curve.

Additionally, mixed liquor (RP-TC-ML Weeks 1–4, C-TC-ML Weeks 5–8, RP-TC-ML Weeks 9–12, C-TC-ML Week 13) and primary effluent (RP-TC-PE Weeks 11–13) samples were subjected to micronutrient analysis. All samples were digested with nitric acid and hydrogen peroxide to dissolve suspended solids, per USEPA method 3050B. Micronutrients, as defined by Jenkins *et al.* (2004), were analysed using inductively coupled plasma mass spectroscopy (ICP-MS) and included calcium (Ca^{2+}), magnesium (Mg^{2+}), potassium (K^{+}), sodium (Na^{+}), manganese (Mn^{2+}), iron (Fe^{3+}) and zinc (Zn^{2+}).

Routine TTF measurements by plant staff were supplemented with measurement of specific resistance to filtration (SRF), a filtering procedure that quantifies the resistance of filtrate passing through a biocake (Scholes *et al.* 2016). The mechanical setup consisted of a glass vacuum filter holder attached to a graduated cylinder. Polycarbonate filters (Millipore Sigma) with a 0.8 μm pore size were used to retain as much flocculated and dispersed biomass as possible (Ng & Hermanowicz 2005). The polycarbonate filter was chosen to best match the hydrophilic properties of the ZeeWeed membrane fibers. The filtering arrangement was attached to a vacuum pump with a constant operating pressure of 10 inches Hg (33.9 kPa). Baseline measurements were taken using unaltered TCRWWTP primary effluent and mixed liquor from the aerobic zone (SRF-TC-PE 1–5, SRF-TC-ML 1–5). SRF was also measured on MBR mixed liquor samples (SRF-DUN-ML 1–2) from the Dundee Wastewater Plant (Dundee, MI), a plant not experiencing the difficulties occurring the TCRWWTP. Biocake SRF values were calculated for both plants using the equation derived in Christensen & Dick (1985) for mixed liquor solutions spiked with Na^+ and Ca^{2+} (23, 46, 115, 230 and 460 mg/L Na^+ , and 40, 80, 200, 400 and 800 mg/L Ca^{2+} , respectively), similar to the experimental framework of Novak *et al.* (1998). Finally, a time-dependent SRF study was completed using a mixture of 200 mL mixed liquor and 50 mL primary effluent from the TCRWWTP. After 3 h, 0.5 mL of a 20 g/L Ca^{2+} solution was added and SRF was tested intermittently and over an 18-h timespan.

RESULTS AND DISCUSSION

MBR fouling often displays several characteristic symptoms, such as permeability loss, TMP increase, increased TTF and higher SRF, all of which were witnessed at the TCRWWTP (Kimura *et al.* 2005). Each of these perpetuate loss to filtering and treatment capacity in the plant. The known physiochemical mechanisms of MBR fouling can occur both on the surface and in the pores of the membrane. Researchers will often categorize MBR disfunction according to the mechanism driving the fouling: cake-layer and gel-layer build-up, surface charge adsorption and pore obstruction, which are common mechanisms that involve various chemical or biological constituents (Lin *et al.* 2014). The difficulty in starting the investigation at TCRWWTP was a lack of compelling evidence identifying a clear fouling mechanism to implicate for the reduced permeability events. Plant

personnel had qualitative evidence, photographs of a seemingly novel Gram-positive organism that appeared, and also observed slime formation; nevertheless, it was unclear to what extent specific microbiological and chemical factors were driving the observed effects. Therefore, we initially explored a hypothesis that involved identifying the gram-positive microorganisms.

Evaluating hypothesis 1: problem microorganisms are driving permeability decline

Among the fourteen isolates submitted for 16S rRNA gene DNA sequence, three Gram-positive genera were identified most frequently in NCBI BLAST with the highest percentage identity (>97%) and no random database matches (E-Value = 0): *Staphylococcus*, *Microbacterium* and *Micrococcus*. All three organisms are ubiquitous in the environment, particularly sewage (Götz *et al.* 2006; Kim *et al.* 2011). Next, we used FISH on samples from TCRWWTP to visualize the selected isolates in the mixed liquor to determine if they had the comma-shaped morphology under *in situ* growth conditions. FISH images with *Staphylococcus*-specific probes show a comma-shaped morphology that matched what was seen and documented by TCRWWTP staff during periods of permeability decline (Figure 2). *Staphylococcus* is a genus of facultative anaerobes whose species are known to contour into irregular morphologies based on environmental stressors, and whose genomes encode for capsular polysaccharide production (Stingele *et al.* 1996; García-Lara *et al.* 2015). With this evidence, we initially concluded that *Staphylococcus* represents the genus of the problem-indicating organisms, and more information was needed on its role in conjunction with permeability upsets.

Annotated Illumina MiSeq 16S rRNA gene analysis (see Table SI-III, Supplementary Information) revealed the presence and relative abundance of *Staphylococcus* within the larger activated sludge community. OTU 0910 matches the sequence of the *Staphylococcus* isolate (100% similarity, see Figure SI-I, Supplementary Information). Other OTUs from the *Staphylococcaceae* family found in the mixed liquor (specifically, those annotated as genera *Macrococcus* and *Jeotgaliococcus*) did not align with the *Staphylococcus* isolate Sanger sequences. When evaluating samples RP-TC-ML Weeks 1–4 and C-TC-ML Weeks 5–8, the relative abundance of OTU 0910 *Staphylococcus* was very low (ranging between 0% and 0.012%) for all samples and were not different between upset and control conditions after evaluation with a non-parametric Wilcoxon signed-rank test (p -value = 0.77). Therefore, we could not discern a correlation

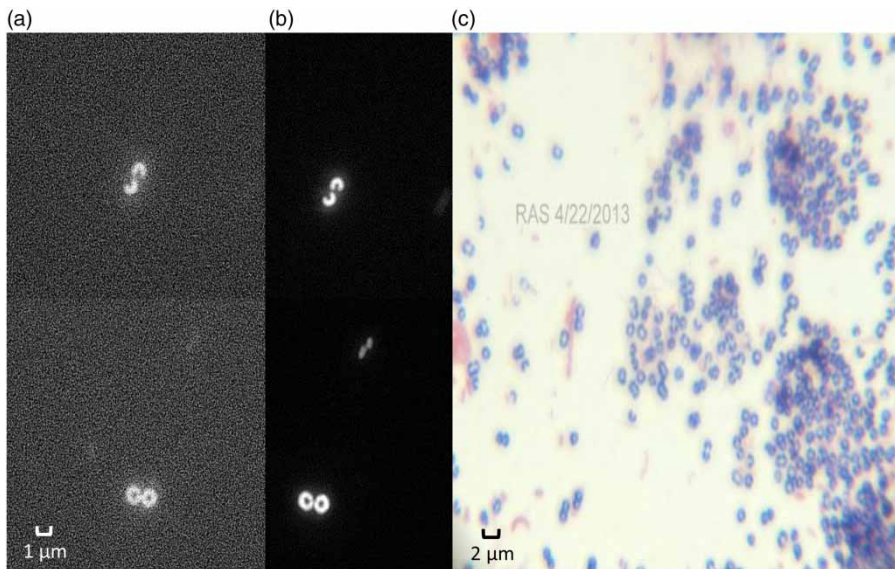


Figure 2 | Fluorescent microscopy of MBR mixed liquor sample using (a) *Staphylococcus*-specific FISH probe and (b) universal DAPI stain from 2017 mixed liquor sample. (c) Gram stain with observed dispersed bacteria during a low permeability upset event in 2013.

between the suspected problematic comma-shaped *Staphylococcus* and permeability decline.

Whole community 16S rRNA gene sequencing analysis revealed the extent to which declining permeability events are unique. At the phylum-level, the relative abundance of *Firmicutes* (the phylum containing the genus *Staphylococcus*) decreased from an average of 31% during the permeability decline in spring 2017 (sample IDs RP-TC-ML-Weeks 1–4) to 11% for the control event (samples C-TC-ML-Weeks 5–8) (see Figure SI-II). When looking at the overall bacterial community, this decrease in *Firmicutes* equates to higher diversity in the control samples (Shannon Index = 0.68–0.71), whereas samples RP-TC-ML-Weeks 1–4 are less diverse (Shannon Index = 0.54–0.6) with *Firmicutes* being one of the most dominant phyla in the community. It is also interesting that samples from January 2018 (RP-TC-ML-Weeks 9–12) have a low relative abundance of *Firmicutes* (5.5%) and a similar diversity index as the control (0.69–0.71). Nevertheless, both samples from reduced permeability events deviate widely in community composition from the control sample and each other (PERMANOVA = 0.001). This result seems to reinforce the idea that treatment plant conditions are different between periods of stable operation and upset, which manifests into unique bacterial community composition. However, because the microbial community structure during each of the declining permeability events was also different, this challenges the initial expectation that a particular microbiological composition would correlate with episodes of permeability decline.

Although we cannot conclude that bacterial composition plays a role in indicating permeability decline, our inability to detect a change in OTU 0910 across upset and control periods weakens the hypothesis that comma-shaped *Staphylococcus* is directly causing the treatment plant upsets. Rather, our data suggest that: (1) the *Staphylococcus* organisms stably exist in the mixed liquor, and (2) growth of comma-shaped bacteria as observed by the operational staff during upset events is an indicator of upset events, either due to changes in the influent or within the bioreactor. Plant personnel observed that the comma-shaped bacteria formed clusters in the plant's return activated sludge, and at the climax of upset events those clusters released planktonic cells into the bulk liquid. Because of this apparent change, it is emphasized that *Staphylococcus* and their Gram-positive relatives are helpful early warning indicators for plant operators of impending upsets. This conclusion led us to acquire new data to support the development of a revised hypothesis concerning factors driving the upsets.

Additional mixed liquor and operating/performance characteristics were obtained to inform the development of hypothesis 2

Carbohydrate:protein characterization

Additional emphasis was placed on unmeasured aspects of TCRWWTP that could elucidate the basis for permeability

decline. Because the treatment plant operators observed slime formation during upset events, experiments were initiated to characterize the carbohydrate and protein concentrations of TCRWWTP's mixed liquor. Traditional knowledge of activated sludge systems states that viscous bulking conditions can occur when carbohydrates are overproduced (Jenkins *et al.* 2004). Indeed, the total carbohydrate fraction in mixed liquor samples was higher ($p = 4.9 \times 10^{-15}$) during the period of declining permeability in spring 2017 (RP-TC-ML Weeks 1–4) than in unstressed control samples (C-TC-ML Weeks 5–8) (Table 1). Protein content, which was relatively stable with a coefficient of variation between all sample reads of 9.6%, was also measured as a representative indicator of biomass.

Ratios of total carbohydrates to total protein during the period of permeability decline in spring 2017 were found to be slightly higher, on average, compared to the control ($p = 7.6 \times 10^{-3}$). Complex carbohydrates (polysaccharides) have been known to negatively affect activated sludge systems through slime formation, or zoogeal or nonfilamentous bulking (Jenkins *et al.* 2004). These conditions can cause fouling and decreased permeability in MBR systems (Hamedi *et al.* 2019). Starting in 2011 and onward, TCRWWTP personnel observed that the membrane surfaces were slimy during critical permeability upsets. The reduced permeability mixed liquor samples also appeared to be more uniformly viscous and had small, dense floc particles compared to larger, easily settleable particles from the control samples. From a functional standpoint, it is logical that a sticky, carbohydrate-rich mixed liquor environment could create or facilitate a more impermeable biocake on the membrane surface.

Table 1 | Mixed liquor assessment of carbohydrate:protein ratio during a reduced permeability period (March/April 2017) and during normal operation (August/September 2017)

Sample ID	Total carbohydrate conc. (mg/L)	Total protein conc. (mg/L)	Ratio (carb/protein)	Avg.
RP-TC-ML-Week 1	234	1,510	0.16	0.16
RP-TC-ML-Week 2	248	1,510	0.16	
RP-TC-ML-Week 3	285	1,750	0.16	
RP-TC-ML-Week 4	252	1,790	0.14	
C-TC-ML-Week 5	216	1,480	0.15	0.12
C-TC-ML-Week 6	139	1,580	0.09	
C-TC-ML-Week 7	175	1,330	0.13	
C-TC-ML-Week 8	190	1,420	0.13	

Carbohydrate concentrations in MBR mixed liquor are often attributed to mixed liquor extracellular polymeric substances (EPS), which is a well-researched component of membrane fouling. EPS production is known to be stimulated for many different reasons, including bacterial signalling, biofilm creation and nutrient accumulation, among others. (Lin *et al.* 2014; Meng *et al.* 2017). Strong evidence exists to suggest that EPS is significantly linked to physical-chemical membrane fouling mechanisms (Lin *et al.* 2014; Jørgensen *et al.* 2017); however, the relationship of EPS and the changing nature of the TCRWWTP mixed liquor in this study was not fully understood.

C:N ratio

The C:N ratio is another important parameter impacting wastewater treatment systems. Wastewater streams contain dissolved, colloidal and particulate matter, including both organics and inorganics, which can blend together to create unfavourable environments that drive fouling mechanisms (Meng *et al.* 2017). As with all wastewater technologies, a proper balance of the ever-changing mass loads to an MBR system is required to stimulate microbial metabolism and growth, and satisfy treatment objectives. For MBR mixed liquor, this ratio becomes even more critical to keep EPS production at healthy levels. C:N imbalances or shock loads to a system have been shown to correlate with membrane fouling events (Wu *et al.* 2012).

When historical plant data were revisited after the spring sampling, we found valuable underlying patterns when the ratios of influent constituents were calculated and plotted, versus plotting the constituents individually. For instance, the BOD₅ to ammonia mass ratio entering the aeration basins through the primary effluent (summarized in Table SI-IV) modestly increased after September 2017 in the lead-up to the permeability event in January 2018, from 5.38 to 6.68 mg BOD₅/mg NH₃-N. The primary effluent BOD₅ to TSS ratio noticeably dropped just before the upset in December/January 2018 from 1.62 to 1.09 mg BOD₅/mg TSS (Figure SI-IV). Analysis of operational data from separate events from 2011, 2012 and 2013 also revealed a variable BOD₅ to ammonia ratio relative to the amount of suspended solids in the system. Data from an upset in 2013, which was particularly troublesome, was reviewed, and a sustained elevated BOD₅ to ammonia ratio (8.11 mg BOD₅/mg TSS on average) in the primary effluent was noticed two weeks before the beginning of the observed permeability decline (see Figures SI-V and SI-VI). The same ratio for August 2018 would seem to negate the

previous pattern, but this appears to be an outlier when viewed with the full data set for the rest of the year (Table SI-IV).

It is possible that a shock load of organic matter could be continuously disrupting the MBR. A sudden change in the food to microorganism ratio (F/M) causes rapid metabolism and production of bound EPS constituents in the mixed liquor (Hamed *et al.* 2019). Results from Xin *et al.* (2014) validate the idea of increased cake-layer resistance after feeding long-chain polysaccharides, specifically alginate, to a membrane system. The higher BOD₅ to ammonia and BOD₅ to TSS ratios suggest that the industrial fraction of the influent may be changing just before a plant disruption. Samples were not collected that could be used to identify the form of organic entering the plant during disruptive periods. Nevertheless, revisiting the influent data allowed us to characterize the baseline, within which individual constituents were changing relative to each other. The outcome of this modified analysis, compared to solely viewing changes to individual mass loadings, implies that permeability issues at TCRWWTP are not attributed to a single influent constituent; rather, a confluence of different constituents perhaps industrial or non-domestic in nature, could be driving mixed liquor quality deterioration.

Monovalent:divalent cationic ratios

The connection between the utility's observation of slime production and the measured increase in the carbohydrate:protein ratio during and after permeability events offered a possible hint about the mechanism of membrane permeability reduction. Slime is often tied to micronutrient deficiencies caused by insufficient cationic inorganic salts, such as Na⁺, K⁺, Ca²⁺ and Mg²⁺ (Jenkins *et al.* 2004). We measured high baseline average total Na⁺ and Ca²⁺ concentrations (106 and 129 mg/L, respectively), and adequate average total Mg²⁺ and K⁺ concentrations (33.3 and 51.9 mg/L, respectively) in the treatment plant's aeration basin during normal operation (samples C-TC-ML-Weeks 5–8, C-TC-ML Week 13, C-TC-ML Weeks 22–23). The required total concentration of these salts for bacterial growth were calculated to be 12.5 mg/L Na⁺, 41.6 mg/L Ca²⁺, 29.1 mg/L Mg²⁺ and 41.6 mg/L K⁺ based on the MLSS and stoichiometric parameters in Grady *et al.* (2011). Concentrations of Mn²⁺, Fe³⁺, and Zn²⁺ were also above the threshold for bacterial growth, which ultimately dismissed micronutrient deficiency as a prevailing factor. In fact, ICP-MS data from mixed liquor samples in 2017 showed that perhaps the opposite was occurring. For the

first period of permeability decline (RP-TC-ML Weeks 1–4), high levels of total Ca²⁺ (between 175 and 278 mg/L) were detected in the mixed liquor (Table SI-V for full detail). During the same time period, Traverse City's drinking water treatment had less than 34 mg/L Ca²⁺, on average, suggesting the remaining mass fraction came from external industrial or domestic sources. The concentrations of total Ca²⁺ during the March/April 2017 TCRWWTP reduced permeability period were found to be significantly higher ($p = 0.045$) than the control samples taken several months later in August/September 2017.

Inorganics are known to have a direct effect on biocake permeability, specifically manifested in deteriorating sludge dewatering quality (Novak *et al.* 1998). According to Higgins & Novak (1997), elevated monovalent cations (Na⁺ and K⁺) in activated sludge wastewater treatment systems result in deflocculation and interfere with liquid–solids separation. In contrast, they showed that divalent cations help consolidate flocs and improve liquid–solids separation. Activated sludge dewatering characteristics are frequently measured by resistance to water passage through an activated sludge cake, which serves as a surrogate for resistance to permeability through an MBR biocake. The work by Higgins & Novak (1997) formed the basis for today's standard recommendation to keep the monovalent-to-divalent cation ratio (milliequivalent-to-milliequivalent, designated M:D ratio) below 1:1 to achieve adequate activated sludge dewaterability (Higgins & Novak, 1997). At TCRWWTP, the M:D ratio of the mixed liquor averages 0.83:1, less than the 1:1 recommended by Higgins & Novak, regardless of permeability issues. The high Ca²⁺ levels experienced during the first week of the permeability upset drove the ratio down to 0.45:1, and then modestly increased over the remaining three weeks, but remained far less than the control period and the other periods of reduced permeability in January 2018. In contrast, several studies concerning calcium fouling mechanisms show increased resistance to filtration coinciding with calcium bridging to different types of polysaccharides at total Ca²⁺ concentrations ranging from 13.3–133 mg/L indicating polymer deposition, up to 240 mg/L indicating gel-layer formation (Xin *et al.* 2014; Miao *et al.* 2018). The concentrations for March 2017 are most similar to the latter; however, over the January 2018 (RP-TC-ML Weeks 9–12) period of permeability decline, total Ca²⁺ concentrations were indistinguishable from the control (128 versus 130 mg/L, respectively) ($p = 0.75$). This would seem to contradict the notion that Ca²⁺-induced gel formation caused the

treatment plant's permeability problems under all conditions. These observations, together with changing mixed liquor and influent characteristics, again imply that the permeability stress experienced by the TCRWWTP MBR cannot be consistently attributed to a single factor, but may be related to a combination of inorganic and organic constituents.

Hypothesis 2: complex interactions of chemical components are driving permeability decline

Consideration of the above led to a general hypothesis involving both high inorganic and organic constituents causing sludge deflocculation and polymer bridging. The question remained whether the permeability upsets at TCRWWTP were the result of two different mechanisms: one due solely to high Ca^{2+} concentration inducing gel formation with organics found native to the mixed liquor; the other relating to external organic loads and subsequent Ca^{2+} polymer bridging. On this basis, we evaluated whether our

data supported Ca^{2+} as the primary cation causing polymer bridging in the MBR system at TCRWWTP, or if another pattern of fouling emerged that included an organic component.

Support of the hypothesis that organic loading and Ca^{2+} -mediated bridging was dependent on the coordination of data from biological and chemical data sets. A constrained ordination plot (Figure 3) of the OTU variance from the MiSeq Illumina reads shows three clusters of communities from the three sampling periods in 2017 and 2018. The variance calculation is developed from the PERMANOVA statistical analysis described previously, but visually shows just how distinct the biological variance is within these three sample groups. Overlapped with the biological variance are chemical concentrations from ICP-MS and TCRWWTP operational metadata from the same time. The direction and magnitude of the arrows point towards objects with similar variance and are considered closely correlated. What is apparent is the correlation of variance between total mixed liquor

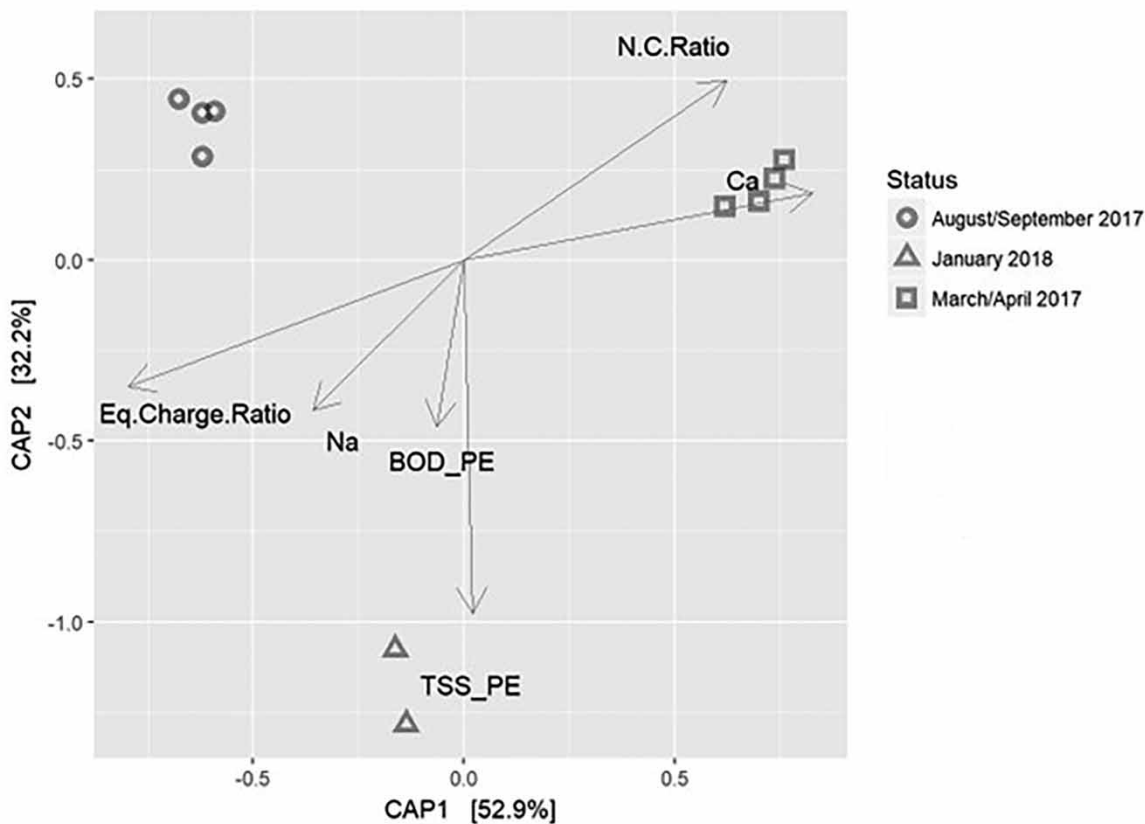


Figure 3 | Constrained ordination plot of TCRWWTP mixed liquor OTU variance and statistical variance of operational metadata – primary effluent nitrogen:carbon ratio (N.C.Ratio), primary effluent BOD (BOD_PE), primary effluent suspended solids (TSS_PE), mixed liquor total calcium concentration (Ca), mixed liquor sodium concentration (Na), mixed liquor equivalence charge ratio (Eq.Charge.Ratio).

Ca^{2+} concentrations and the mixed liquor microbiology from March and April 2017. In January, the community variance appears to be related to high levels of primary effluent suspended solids, which is reinforced by the operational data at that time. This strengthens the proposition that a unique set of carbonaceous and inorganic nutrient concentrations in the system mixed liquor has been dictating microbiological response, causing irregularities in morphology, dispersal of organisms and production of carbohydrate-rich EPS.

Preliminary evaluation of membrane resistance supports alternative hypothesis 2

The hypothesis that increased Ca^{2+} resulted in adverse changes to mixed liquor filtration characteristics was tested by controlled addition of Ca^{2+} to TCRWWTP mixed liquor, followed by SRF measurement (samples SRF-TC-ML 6–8). Regular mixed liquor from TCRWWTP filtered well (Figure 4), with an average SRF value of 1.3×10^{12} m/kg, but increased steadily with increasing Ca^{2+} ion addition.

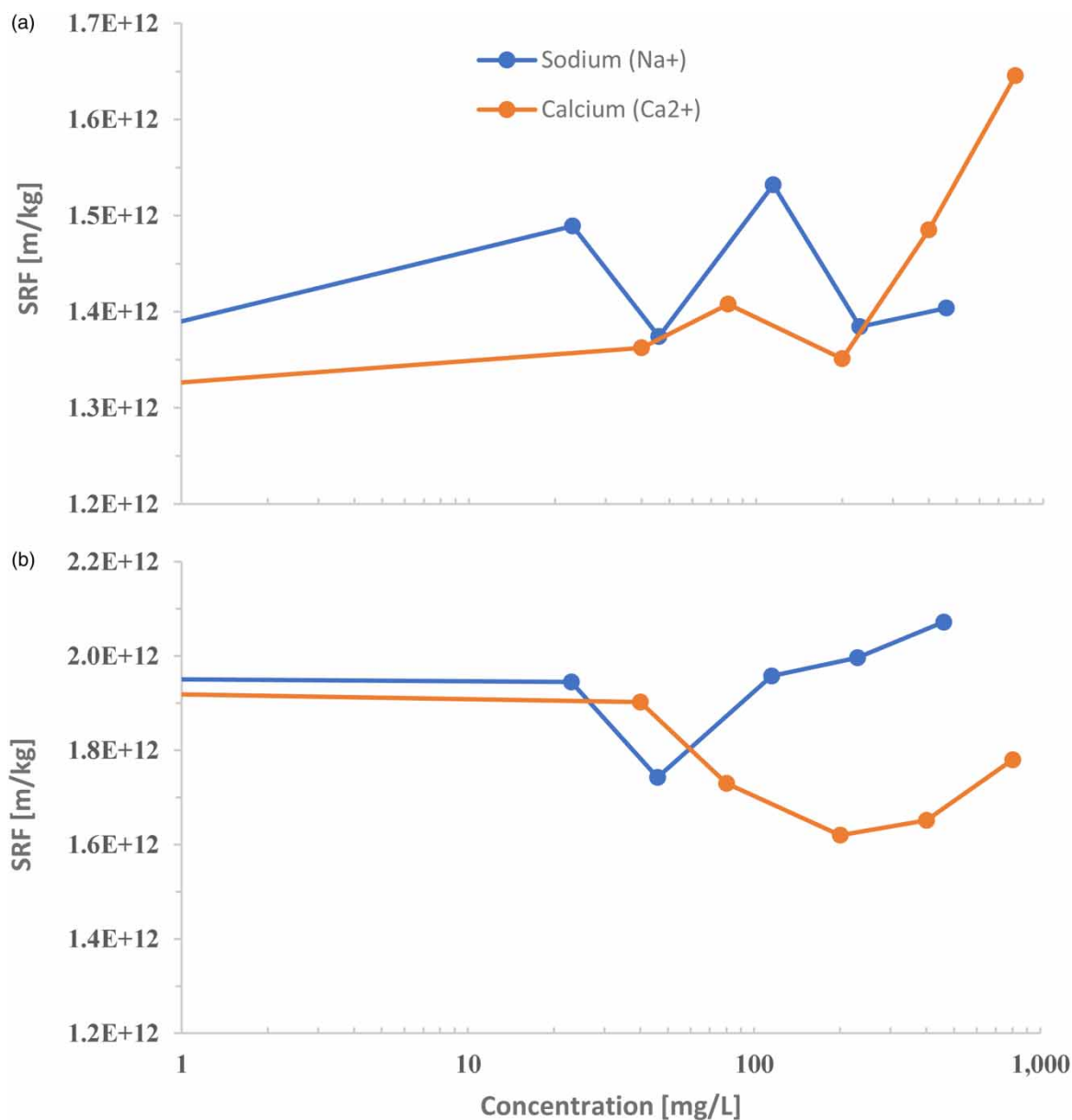


Figure 4 | Comparison of TCRWWTP (a) and Dundee Wastewater Plant (b) SRF values with increasing sodium and calcium concentrations.

After the addition of 800 mg/L Ca^{2+} , SRF values increased nearly 25% over the ML baseline. Na^+ additions to the mixed liquor had variable impact to biocake SRF, but with a general positive correlation with slightly higher resistance values. These results demonstrate a negative effect on biocake permeability relative to the cation concentration in the mixed liquor, but the magnitude of the changes to SRF was lower than expected. This could explain why plant personnel noted in March 2017, when mixed liquor total Ca^{2+} concentrations were 278 mg/L, that permeability was not impacted as greatly as other upsets seen in the past or the upset experienced in January 2018.

In comparison (Figure 4), the exact same filterability experiment using mixed liquor from Dundee Wastewater Plant had opposite results. The Dundee mixed liquor resistance to filtrations decreased with the same spiked additions of Ca^{2+} . The addition of Na^+ caused a minor deterioration in filterability, which agrees with the results from Higgins & Novak (1997). However, in direct contrast to TCRWWTP measurements, Dundee's baseline mixed liquor total Ca^{2+} concentration was higher than TCRWWTP at 281 mg/L. As the polymer bridging studies in Xin *et al.* (2014) demonstrate, total Ca^{2+} concentrations exceeding 280 mg/L have dramatic decreases in cake resistance, solution viscosity and filtration times due to the formation of porous aggregates. This probably explains the high mixed liquor baseline SRF value of 1.94×10^{12} and subsequent decline with additional Ca^{2+} . It would appear that the TCRWWTP mix has a unique quality when normal Ca^{2+} concentrations exist near the threshold for cationic saturation of polymer binding sites to induce a gel formation, but diverges from literature expectations, with any additional Ca^{2+} loads past this threshold continuing to be detrimental to biocake permeability.

Preliminary SRF tests were conducted to uncover the extreme permeability events of January 2018 by taking SRF values after additions of both organic matter from the primary effluent and inorganics through spiked additions of Ca^{2+} . Ultimately, SRF values were found to substantially increase over time: a resistance measurement over $\times 10$ that of a fresh mixed liquor sample was seen after 18 h of mixing. This also marked a considerable increase over the Ca^{2+} spiked addition values discussed above (see SI Section 3 and Figure SI-VIII for details and results). More testing is required with samples from known locations to establish a connection to the source of problem organic matter.

Continuing work

Subsequent to the experimental laboratory investigation, TCRWWTP began routine sampling in July 2018 of influent wastewater (C-TC-INF Weeks 14–23) to analyse total and filtered chemical oxygen demand and total and filtered carbohydrates (Standard Methods; DuBois Method, described previously). In April 2019, this sample regimen was extended to significant industrial customers that are known to contribute higher strength wastewater to the plant collection system (C-SIU-EFF Weeks 22–23). Knowledge of what to look for in terms of carbon and macronutrient inconsistencies will give plant personnel a better understanding of external effects on the plant influent and mixed liquor quality. Samples from targeted collection system outfalls, plant influent and plant mixed liquor will be compiled into one mass balance with the goal of understanding sources of organic and inorganic sources. As a practical step towards day-to-day monitoring of influent cations, a conductance probe was installed at the headworks to the plant, and routine samples are collected for ICP-MS quantification.

CONCLUSIONS

This study investigated the contribution of chemical and biological factors at a full-scale MBR plant experiencing periods of sudden permeability decline. At the onset of experimentation, it was believed that dispersed organisms were the root cause. The organisms were the most apparent visual link to permeability decline because of their unmistakable growth pattern, but were ultimately not found to be a principal cause of permeability decline at TCRWWTP. However, increased *Staphylococcus* appearance in mixed liquor samples will continue to be a useful tool for indicating an impending upset. Chemical analysis and filtration characteristics showed the mixed liquor response to Ca^{2+} and Na^+ additions was different from normal operations, and opposite to the response from another MBR wastewater treatment plant treating largely municipal wastewater.

A compliment of data and analysis suggests that permeability decreases at the TCRWWTP occur when a combination of inorganic (principally calcium) and organic constituents are present in the plant influent wastewater. There is evidence to suggest that the organics are from non-domestic sources. The exact makeup of these flows is unknown; however, plant staff are using the techniques

identified through this study to identify potential sources of the constituents that cause periodic permeability upsets.

ACKNOWLEDGEMENTS

This study was funded by the Traverse City Regional Wastewater Treatment Plant (Jacobs). We thank Dr Alex Rosenthal for his contributions and expertise in assisting with the FISH hybridization and fluorescent microscopy. We are also grateful to Dave Rigel at the Dundee Wastewater Treatment Plant for assistance in obtaining samples.

DATA AVAILABILITY STATEMENT

All relevant data are included in the paper or its Supplementary Information.

REFERENCES

- Blair, S. 2012 Investigation into Causes of a permeability crisis at large membrane bioreactor. In: *Proceedings of the Water Environment Federation, Alexandria, VA 22314-1994, USA*. <https://www.accesswater.org/?id=-281088>. Accessed 31 March 2019.
- Chiao, T., Clancy, T. M., Pinto, A., Xi, C. & Raskin, L. 2014 Differential resistance of drinking water bacterial populations to monochloramine disinfection. *Environmental Science & Technology* **48**, 4038–4047. <https://doi.org/10.1021/es4055725>.
- Christensen, B. G. L. & Dick, R. I. 1985 Specific resistance measurements: methods and procedures. *Journal of Environmental Engineering* **111** (3), 258–271.
- Cole, J. R., Wang, Q., Fish, J. A., Chai, B., McGarrell, D. M., Sun, Y., Brown, C. T., Porras-Alfaro, A., Kuske, C. R. & Tiedje, J. M. 2014 Ribosomal database project: data and tools for high throughput rRNA analysis. *Nucleic Acids Research* **42**, D633–D642. doi: 10.1093/nar/gkt1244.
- DuBois, M., Gilles, K. A., Hamilton, J. K., Rebers, P. A. & Smith, F. 1956 Colorimetric method for determination of sugars and related substances. *Analytical Chemistry* **28** (3), 350–356.
- García-Lara, J., Weihs, F., Ma, X., Walker, L., Chaudhuri, R. R., Kasturiarachchi, J., Crossley, H., Golestanian, R. & Foster, S. J. 2015 Supramolecular structure in the membrane of *Staphylococcus aureus*. *Proceedings of the National Academy of Sciences* 201509557. <https://doi.org/10.1073/pnas.1509557112>.
- Götz, F., Bannerman, T. & Schleifer, K. 2006 *The Genera Staphylococcus and Micrococcus. The Prokaryotes (Vol. 4)*. https://doi.org/10.1007/0-387-30744.3_1.
- Grady Jr, L., Daigger, G. T., Love, N. G. & Filipe, C. D. M. 2011 *Biological Wastewater Treatment*, 3rd edn, CRC Press, Boca Raton, FL.
- Hamed, H., Ehteshami, M., Mirbagheri, S. A., Rasouli, S. A. & Zendejboudi, S. 2019 Current status and future prospects of membrane bioreactors (MBRs) and fouling phenomena: a systematic review. *The Canadian Journal of Chemical Engineering* **97**, 32–58. <https://doi.org/10.1002/cjce.23345>.
- Higgins, M. J. & Novak, J. T. 1997 Dewatering and settling of activated sludges: the case for using cation analysis. *Water Environment Research* **69** (2), 225–232.
- Hill, V. R., Narayanan, J., Gallen, R. R., Ferdinand, K. L., Cromeans, T. & Vinjé, J. 2015 Development of a nucleic acid extraction procedure for simultaneous recovery of DNA and RNA from diverse microbes in water. *Pathogens* **4** (2), 335–354.
- Jenkins, D., Richard, M. G. & Daigger, G. T. 2004 *Manual on the Causes and Control of Activated Sludge Bulking and Foaming and Other Solids Separation Problems*, 3rd edn. CRC Press, London, UK
- Jørgensen, M. K., Nierychlo, M., Nielsen, A. H., Larsen, P., Christensen, M. L. & Nielsen, P. H. 2017 Unified understanding of physico-chemical properties of activated sludge and fouling propensity. *Water Research* **120**, 117–132. <https://doi.org/10.1016/j.watres.2017.04.056>.
- Kim, D. W., Heinze, T. M., Kim, B. S., Schnackenberg, L. K., Woodling, K. A. & Sutherland, J. B. 2011 Modification of norfloxacin by a *Microbacterium* sp. strain isolated from a wastewater treatment plant. *Applied and Environmental Microbiology* **77** (17), 6100–6108. <https://doi.org/10.1128/AEM.00545-11>.
- Kimura, K., Yamato, N., Yamamura, H. & Watanabe, Y. 2005 Membrane fouling in pilot-scale membrane bioreactors (MBRs) treating municipal wastewater. *Environmental Science and Technology* **39** (16), 6293–6299. <https://doi.org/10.1021/es0502425>.
- Kozich, J. J., Westcott, S. L., Baxter, N. T., Highlander, S. K. & Schloss, P. D. 2013 Development of a dual-index sequencing strategy and curation pipeline for analyzing amplicon sequence data on the MiSeq Illumina sequencing platform. *Applied and Environmental Microbiology* **79** (17), 5112–5120.
- Lesjean, B., Gnirss, R. & Adam, C. 2002 Process configurations adapted to membrane bioreactors for enhanced biological phosphorous and nitrogen removal. *Desalination* **149** (1–3), 217–224. [https://doi.org/10.1016/S0011-9164\(02\)00762-2](https://doi.org/10.1016/S0011-9164(02)00762-2).
- Lin, H., Zhang, M., Wang, F., Meng, F., Liao, B., Hong, H. & Gao, W. 2014 A critical review of extracellular polymeric substances (EPSs) in membrane bioreactors: characteristics, roles in membrane fouling and control strategies. *Journal of Membrane Science* **460**, 110–125. <https://doi.org/10.1016/j.memsci.2014.02.034>.
- Lowry, O. H., Rosebrough, N. J., Farr, A. L. & Randall, R. J. 1951 Protein measurement with the folin phenol reagent. *Journal of Biological Chemistry* **193** (1), 265–275.
- Meng, F., Zhang, S., Oh, Y., Zhou, Z., Shin, H. S. & Chae, S. R. 2017 Fouling in membrane bioreactors: an updated review.

- Water Research* **114**, 151–180. <https://doi.org/10.1016/j.watres.2017.02.006>.
- Miao, R., Wu, Y., Wang, P., Wu, G., Wang, L., Li, X., Wang, J., Lv, Y. & Liu, T. 2018 New insights into the humic acid fouling mechanism of ultrafiltration membranes for different Ca²⁺ dosage ranges: results from micro- and macro-level analyses. *Water Science and Technology*. wst2018141. <https://doi.org/10.2166/wst.2018.141>
- Miller, D. N., Bryant, J. E., Madsen, E. L. & Ghiorse, W. C. 1999 Evaluation and optimization of DNA extraction and purification procedures for soil and sediment samples. *Applied and Environmental Microbiology* **65** (11), 4715–4724.
- Ng, H. Y. & Hermanowicz, S. W. 2005 Specific resistance to filtration of biomass from membrane bioreactor reactor and activated sludge. *Water Environment Research* **77** (2), 187–192.
- Nielsen, P. H., Daims, H., Lemmer, H., Arslan-Alaton, I. & Olmez-Hanci, T. 2009 *FISH Handbook for Biological Wastewater Treatment*. IWA Publishing, London.
- Novak, J. T., Love, N. G., Smith, M. L. & Wheeler, E. R. 1998 The effect of cationic salt addition on the settling and dewatering properties of an industrial activated sludge. *Water Environment Research* **70** (5), 984–996.
- Pruesse, E., Quast, C., Knittel, K., Fuchs, B. M., Ludwig, W., Peplies, J. & Glöckner, F. O. 2007 SILVA: a comprehensive online resource for quality checked and aligned ribosomal RNA sequence data compatible with ARB. *Nucleic Acids Research* **35** (21), 7188–7196.
- Schloss, P. D., Westcott, S. L., Ryabin, T., Hall, J. R., Hartmann, M., Hollister, E. B., Lesniewski, R. A., Oakley, B. B., Parks, D. H., Robinson, C. J., Sahl, J. W., Stres, B., Thallinger, G. G., Van Horn, D. J. & Weber, C. F. 2009 Introducing mothur: open-source, platform-independent, community supported software for describing and comparing microbial communities. *Applied and Environmental Microbiology* **75** (23), 7537.
- Scholes, E., Verheyen, V. & Brook-Carter, P. 2016 A review of practical tools for rapid monitoring of membrane bioreactors. *Water Research* **102**, 252–262. <https://doi.org/10.1016/j.watres.2016.06.031>.
- Standard Methods for the Examination of Water and Wastewater. 2017. 23rd edn, American Public Health Association/American Water Works Association/Water Environment Federation, Washington DC, USA.
- Stingele, F., Neeser, J. R. & Mollet, B. 1996 Identification and characterization of the eps (Exopolysaccharide) gene cluster from *Streptococcus thermophilus* Sfi6. *Journal of Bacteriology* **178** (6), 1680–1690.
- Wright, E. S., Safak Yilmaz, L., Corcoran, A. M., Ökten, H. E. & Noguera, D. R. 2014 Automated design of probes for rRNA-targeted fluorescence in situ hybridization reveals the advantages of using dual probes for accurate identification. *Applied and Environmental Microbiology* **80** (16), 5124–5133. <https://doi.org/10.1128/AEM.01685-14>.
- Wu, B., Yi, S. & Fane, A. G. 2012 Effect of substrate composition (C/N/P ratio) on microbial community and membrane fouling tendency of biomass in membrane bioreactors. *Separation Science and Technology* **47** (3), 440–445. <https://doi.org/10.1080/01496395.2011.621503>.
- Xin, Y., Bligh, M. W., Kinsela, A. S., Wang, Y. & Waite, T. D. 2014 Calcium-mediated polysaccharide gel formation and breakage: impact on membrane foulant hydraulic properties. *Journal of Membrane Science* **475**, 395–405.

First received 7 May 2020; accepted in revised form 20 July 2020. Available online 31 July 2020